

# Effects of black cumin seed oil on oxidative stress and expression of membrane-cytoskeleton linker proteins, radixin, and moesin in streptozotocin-induced diabetic rat liver

Ugur Seker<sup>1</sup>, Seval Kaya<sup>2</sup>, Sevgi Irtegun Kandemir<sup>3</sup>, Dila Sener<sup>4</sup>, Ozlem Unay Demirel<sup>5</sup>, Yusuf Nergiz<sup>2</sup>

<sup>1</sup>Department of Histology and Embryology, Harran University School of Medicine, Sanliurfa, Turkey; <sup>2</sup>Department of Histology and Embryology, Dicle University School of Medicine, Diyarbakir, Turkey; <sup>3</sup>Department of Medical Biology, Dicle University School of Medicine, Diyarbakir, Turkey; <sup>4</sup>Department of Histology and Embryology, Bahcesehir University School of Medicine, Istanbul, Turkey; <sup>5</sup>Department of Medical Biochemistry, Bahcesehir University School of Medicine, Istanbul, Turkey

## Abstract

**Background and Aim:** This study examined the effects of black cumin seed oil treatment on oxidative stress and the expression of radixin and moesin in the liver of experimental diabetic rats.

**Materials and Methods:** Eighteen rats were divided into 3 equal groups (control, diabetes, treatment). The control group was not exposed to any experimental treatment. Streptozotocin was administered to the rats in the diabetes and treatment groups. A 2.5 mL/kg dose of black cumin seed oil was administered daily for 56 days to the treatment group. At the conclusion of the experiment, the blood level of malondialdehyde (MDA) and glutathione (GSH) was measured. The expression level and the cellular distribution of radixin and moesin in the liver were analyzed.

**Results:** The plasma MDA ( $3.05 \pm 0.45$  nmol/mL) and GSH ( $78.49 \pm 20.45$   $\mu$ mol/L) levels in the diabetes group were significantly different ( $p < 0.01$ ) from the levels observed in the control group (MDA:  $1.09 \pm 0.31$  nmol/mL, GSH:  $277.29 \pm 17.02$   $\mu$ mol/L) and the treatment group (MDA:  $1.40 \pm 0.53$  nmol/mL, GSH:  $132.22 \pm 11.81$   $\mu$ mol/L). Immunohistochemistry and western blotting analyses indicated that while the level of radixin was not significantly between the groups ( $p > 0.05$ ) and moesin expression was significantly downregulated ( $p < 0.05$ ) in the experimental group, the treatment was ineffective.

**Conclusion:** The administered dose was sufficient to prevent oxidative stress, but was not sufficient to alleviate the effects of diabetes on moesin expression in hepatic sinusoidal cells.

**Keywords:** Diabetes; liver; moesin; radixin; rat.

## Introduction

Diabetes is one of the most common metabolic diseases worldwide, and the incidence continues to increase. It has been reported that approximately 451 million people suffered from diabetes-related complications in 2017, and that figure is estimated to increase to 693 million by 2045.<sup>[1]</sup> In diabetic conditions, the effects on lipid and protein metabolism can lead to life threatening complications, such as nephropathy, retinopathy, hepatopathy, vasculopathy, and neuropathy.<sup>[2]</sup> Both morphological and biochemical degeneration in liver may be observed. Increased oxidative stress, apoptotic cell death, and an increased level of hepatic enzymes in blood demonstrate reduced organ function and injury. Diabetes-related liver injury has been associated with various cellular mechanisms.<sup>[3-5]</sup> Several experimental studies have been performed to find the optimal treatment method for insulin-dependent diabetic liver injury with the fewest side effects and lowest cost, and the large number diabetes-related articles demonstrate the topicality of the current study. Some of this research has examined the possibility of alleviating streptozotocin (STZ)-induced diabetic complications with herbal medicine. Black cumin (*Nigella sativa*) seed oil and its major compound, thymoquinone, has exhibited anti-hyperglycemic activity in STZ-induced diabetes, and the results have suggested that the treatment had a protective effect on diabetes-related organ complications.<sup>[6,7]</sup> Diabetes can lead to cellular cytoskeleton changes, which may affect cellular functions.<sup>[8]</sup> The cellular skeleton consists of filamentous proteins, including actin filaments, which are cross-linked to the plasma membrane by members of the ezrin-radixin-moesin (ERM) protein family.<sup>[9]</sup> ERM proteins have specific tissue expression levels and functions. For example, radixin is expressed in the liver, and moesin is expressed in the spleen, lungs, kidneys, lymphocytes, and vascular endothelial cells.<sup>[10,11]</sup> Radixin is typically expressed in hepatocytes and bile canaliculi to act as a scaffold protein for multidrug resistance-associated protein 2.<sup>[12]</sup> Previous studies have reported that moesin activates hepatic stellate cells during fibrosis formation in ischemic liver injury.<sup>[13,14]</sup> In diabetes, expression of the third member of the ERM protein family, ezrin, is reduced in podocytes of the kidney. It has been suggested that ERM proteins contribute to the pathogenesis of diabetic nephropathy.<sup>[15]</sup> The available literature on relationships between ERM family members and diabetic liver injury is very limited. The objective of this study was to investigate the effects of black cumin seed oil on oxidative stress status and expression-distribution of the cytoskeletal proteins, radixin and moesin, in the liver of experimental STZ-induced diabetic rats.

**How to cite this article:** Seker U, Kaya S, Irtegun Kandemir S, Sener D, Unay Demirel O, Nergiz Y. Effects of black cumin seed oil on oxidative stress and expression of membrane-cytoskeleton linker proteins, radixin, and moesin in streptozotocin-induced diabetic rat liver. *Hepatology Forum* 2022; 3(1):21–26.

**Received:** September 16, 2021; **Accepted:** November 01, 2021; **Available online:** November 30, 2021

**Corresponding author:** Ugur Seker; Harran Universitesi Tip Fakultesi, Histoloji ve Embriyoloji Anabilim Dalı, Sanliurfa, Turkey  
**Phone:** +90 414 318 30 31; **e-mail:** seker.ugur.tr@gmail.com



OPEN ACCESS  
This work is licensed under a Creative Commons Attribution-NonCommercial 4.0 International License.

© Copyright 2022 by Hepatology Forum - Available online at [www.hepatologyforum.org](http://www.hepatologyforum.org)



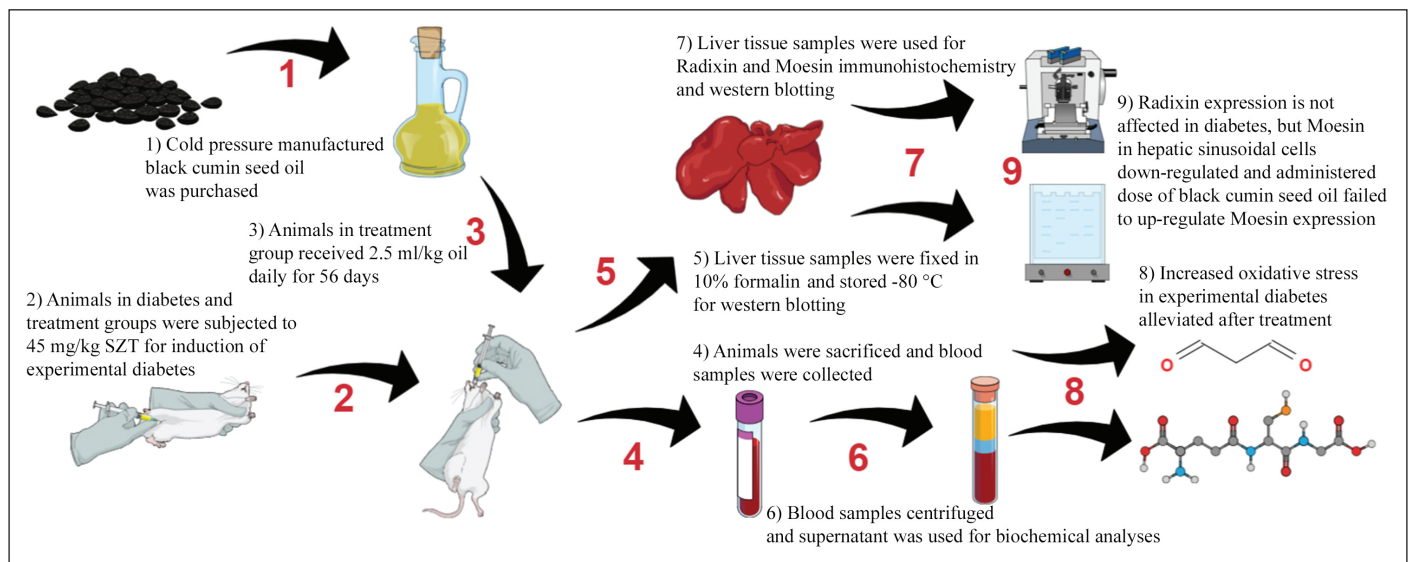


Figure 1. Illustration of the study design protocol and the results.

## Materials and Methods

### Experimental Design

The experimental process used in the study is illustrated in Figure 1. The research was approved by the Local Experimental Animal Ethics Committee of Dicle University (date: 28.03.2019, number: 2019/04), and all of the procedures were performed according to the US National Institutes of Health Guide for the Care and Use of Laboratory Animals (NIH Publications No. 8023, revised 1978). Eighteen adult male Wistar Albino rats weighing  $283.61 \pm 27.93$  g supplied by the Health Sciences Application and Research Center of Dicle University were divided into 3 groups: control (n=6), diabetes (n=6), and treatment (n=6). All of the rats were housed in polycarbonate laboratory animal cages with standard pellet feed and water available ad libitum. Standard room temperature ( $21 \pm 3^\circ\text{C}$ ) and humidity ( $50 \pm 5\%$ ) were maintained, as well as a 12-hour day and night cycle. A 1-week adaption period was observed before beginning the experimental process.

### Induction of Experimental Diabetes

The blood glucose level of the animals was measured from the tail vein with a portable glucometer prior to initiating the experiment. The rats in the control group were not subjected to any treatment and were sacrificed at the conclusion for comparison. A single intraperitoneal injection of 45 mg/kg STZ dissolved in freshly prepared ice-cold 0.1 M citrate buffer was administered to the rats in the diabetes and treatment groups to induce diabetes. Water with 10% glucose was provided ad libitum for 48 hours to avoid hypoglycemia. The blood glucose level was measured 72 hours after the STZ injection and a value of  $>240$  mg/dL was considered diabetic. A daily dose of 2.5 mL/kg of commercially produced black cumin seed oil was orally administered to the rats in the treatment group. Previous research has indicated that this dosage of the plant extract provided anti-hyperglycemic and hepatoprotective effects.<sup>[16,17]</sup> The experiment continued for 56 days following confirmation of experimental diabetes, after which the animals were euthanized. Blood was withdrawn from heart and liver tissue samples and the blood was centrifuged and stored at  $-20^\circ\text{C}$  for further analysis. Excised liver tissue samples were fixed in Bouin's fixative for histopathological examination and frozen at  $-80^\circ\text{C}$  for western blotting.

### Biochemical Analysis

The blood samples were immediately centrifuged at a force of 1370 xg at  $4^\circ\text{C}$  for 10 minutes and the supernatant was carefully collected. The plasma was mixed with thiobarbituric acid and boiled at  $95^\circ\text{C}$  for 30 minutes. In order to measure the level of malondialdehyde (MDA) level, the by-products of lipid peroxidation - thiobarbituric acid reactive substances - were measured using the process described by Yagi et al.<sup>[18]</sup> The extinction coefficient of  $1.56 \times 10^5 \text{ M}^{-1} \text{ cm}^{-1}$  was used to determine the MDA equivalent expressed as nmol/mL. Glutathione (GSH) was measured using a modified version of the protocol previously described using Ellman's reagent. The supernatant was mixed with disodium phosphate dihydrate solution and dithio-bis nitrobenzoic acid. Following thorough mixture, the absorbance was quickly measured at 412 nm. The GSH level was obtained using the  $13,600 \text{ M}^{-1} \text{ cm}^{-1}$  extinction coefficient and the result was expressed as  $\mu\text{mol/L}$ .<sup>[19]</sup>

### Tissue Processing and Immunohistochemistry

The fixed tissue samples were washed under tap water, dehydrated with a successive alcohol series, cleared with 2 series of xylene, and embedded in paraffin. Five- $\mu\text{m}$ -thick sections were obtained using a rotary microtome and deparaffinized with xylene. The samples were rehydrated using an alcohol series, rinsed with distilled water, and immersed in phosphate buffered saline (PBS). After completing the washing steps, the sections were heated in citrate buffer (ph: 6.0) on a hot-plate and maintained at sub-boiling temperature for antigen retrieval. After 10 minutes, the samples were cooled to room temperature and rinsed in 2 series of PBS. Endogenous peroxidase activity was blocked with 3% hydrogen peroxide diluted with methanol. Antibody dilution at a ratio of 1:300 and all of the subsequent immunohistochemical steps were performed according the instructions provided with a ready-to-use kit (cat no: TP-125-HL; Thermo Scientific, Waltham, MA, USA). A 3,3'-diaminobenzidine (DAB) chromogen kit (cat no: TA-125-HD; Thermo Scientific, Waltham, MA, USA) was used to produce immunohistochemical signaling. Tissue sections were counterstained with Harris hematoxyline, mounted with Entellan (Merck, Whitehouse Station, NJ, USA) medium, and visualized under a light microscope with an attached camera (Aixoscope 5, Carl Zeiss NTS, Oberkochen, Germany).

## Western Blotting

Liver samples (60 mg) frozen with liquid nitrogen were pulverized, mixed with 300  $\mu$ L lysis buffer (cat no: 1861284; Thermo Scientific, Waltham, MA, USA), and incubated on ice for 1 hour. The total protein value of each sample was measured with a bicinchoninic acid kit (cat no: 21071; iNtRON Biotechnology, Seongnam, Gyeonggi, South Korea.). The protein lysate was mixed with 2X Laemmli buffer and boiled at 95°C for 5 minutes. A total of 25  $\mu$ g of protein sample was then separated in 10% tris-glycine extended stain-free gel at 200 V for 20 minutes. The separated proteins were transferred to a polyvinylidene fluoride membrane and blocked for 1 hour at room temperature in 5% skim milk dissolved in phosphate buffered saline with Tween (PBS-T) (Tween: ICI Americas, Wilmington, DE, USA). The membranes were incubated with 1:1000 diluted radixin (cat no: ab52495; Abcam, Cambridge, UK), moesin (cat no: ab151542; Abcam, Cambridge, UK), and  $\beta$ -actin (cat no: sc-47778; Santa Cruz Biotechnology, Dallas, TX, USA) antibodies for 2 hours at room temperature. The membranes were washed in PBS-T and incubated with 1:10000 diluted secondary antibodies for 1 hour at room temperature. Immunoblotting was performed using enhanced chemiluminescence substrate (cat no: 1705061; Bio-Rad Laboratories, Hercules, CA, USA). The bands were monitored with chemiluminescence imaging equipment (ChemiDoc MP; Bio-Rad Laboratories, Hercules, CA, USA) and captured with Image Lab 6.1 Software (Bio-Rad Laboratories, Hercules, CA, USA). The intensity of the bands was quantitated using Image-J software Version 1.46 (US National Institutes of Health, Bethesda, MD, USA).

## Threshold Analysis of Immunostaining

Sixteen randomly selected liver lobules containing a central vein were used to quantify the intensity of the antigen in each group and used for threshold analysis. The total lobule and DAB positive areas were measured using Image-J Version 1.46 software, the results were converted to a ratio indicating the immunopositivity intensity for each lobule, and the results were analyzed statistically.

## Immunoblotting Quantification

The immunoblotting band intensity and thickness were analyzed using Image-J Version 1.46 software. The plot lane plug-in was used to measure band intensity within a rectangle. The peak of each plot was enclosed, and the software calculated a percentage automatically. The thickness for each interest protein band was compared according to  $\beta$ -actin band thickness. The measurement was repeated using 3 randomly selected exposure times and the results were analyzed statistically.

## Statistical Analysis

Due to the limited sample size and the distribution of the values of each group, the non-parametric Kruskal-Wallis test was used to evaluate statistical significance. Multiple comparisons between groups were evaluated with Tamhane's T2 test. The results were expressed as mean $\pm$ SD and  $p < 0.05$  was considered significant.

## Results

### Biochemical Analysis

The lowest lipid peroxidation was measured in the control group, and the MDA level demonstrated a significant increase ( $p < 0.01$ ) in the di-

**Table 1.** Statistical analysis of plasma lipid peroxidation and glutathione levels

	Control	Diabetes	Treatment	p
MDA (nmol/mL)	1.09 $\pm$ 0.31 <sup>a</sup>	3.05 $\pm$ 0.45 <sup>b</sup>	1.40 $\pm$ 0.53 <sup>a</sup>	<0.01
GSH ( $\mu$ mol/L)	277.29 $\pm$ 17.02 <sup>c</sup>	78.49 $\pm$ 20.45 <sup>e</sup>	132.22 $\pm$ 11.81 <sup>d</sup>	<0.01

Statistical significance of group comparisons: a, b:  $P < 0.01$ ; c–e  $P < 0.01$ ; GSH: Glutathione; MDA: Malondialdehyde.

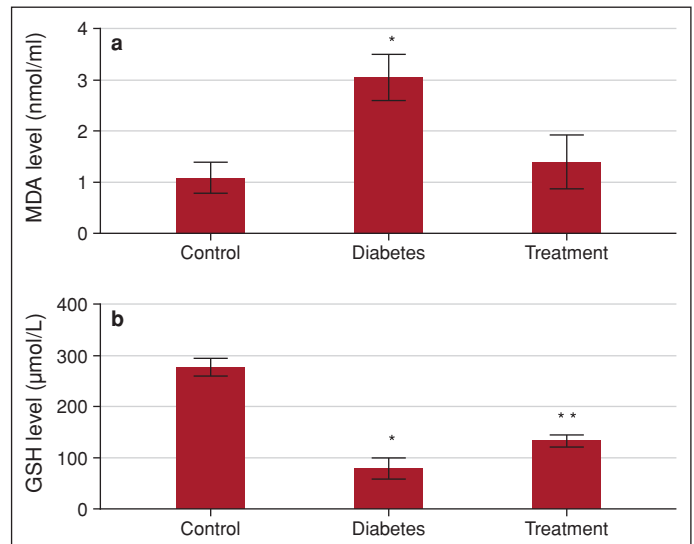


**Figure 2.** Graphical demonstration of (a) plasma lipid peroxidation (malondialdehyde; MDA) and (b) glutathione (GSH) levels. \*:  $P < 0.01$ ; \*\*:  $P < 0.01$ .

abetes group. The mean plasma lipid peroxidation level in the black cumini seed oil-treated animals had declined and was similar to that of the controls ( $p > 0.05$ ). The mean GSH level of the control group was the highest, and it was dramatically lower ( $p < 0.01$ ) in the diabetes group. The mean GSH level of the treatment group was between that of the control and diabetes groups, and the difference was significant ( $p < 0.01$ ). The biochemical analysis results are shown in Table 1 and Figure 2.

### Immunohistochemical and Threshold Analyses Results

Microscopic investigation indicated that hepatocytes were intensely radixin-positive. Immunopositivity was also observed in the sinusoidal endothelial cells and hepatic stellate cells of the control group. In particular, radixin positivity was evident in the plasma membrane, and cytosolic accumulation of this protein was observed in some hepatocytes. The microscopic cellular distribution of radixin in the control, diabetes, and treatment groups was similar (Fig. 3). Threshold analysis of radixin indicated that the positivity was 46.13 $\pm$ 13.61% in the control group, while it was 41.67 $\pm$ 20.99% and 48.66 $\pm$ 14.06% in the diabetes and treatment groups, respectively. The statistical analysis was consistent with light microscopic observations and there was no significant difference between groups ( $p > 0.05$ ). Hepatocytes were observed to be immunonegative for moesin; immunopositivity was only observed in hepatic sinusoidal cells and hepatic stellate cells (Fig. 4). Light microscopic evaluation indicated that the distribution in some hepatic lobules differed significantly between groups. The result of threshold analysis of moesin in the control group was 9.37 $\pm$ 3.08%. Moesin immunopositiv-



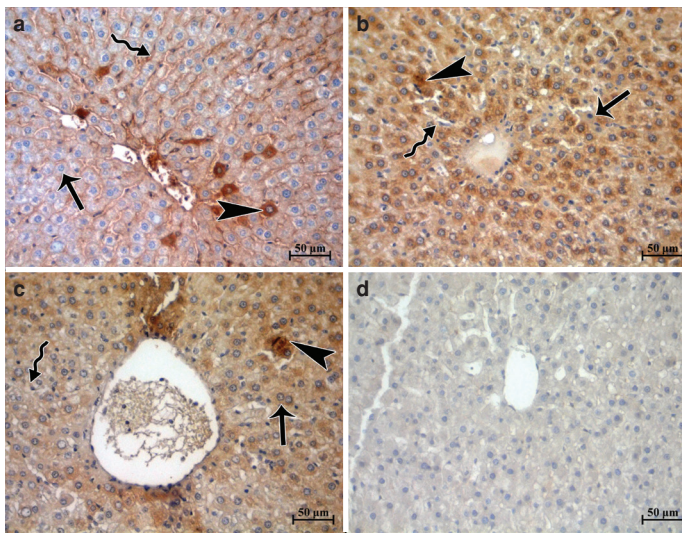


**Figure 3.** Representative micrographs of radixin in the (a) control, (b) diabetes, and (c) treatment groups, as well as (d) negative control. Radixin immunopositivity in the hepatocyte membrane (arrow), accumulation of radixin in the cytosol of some hepatocytes (arrowhead), and immunopositivity in sinusoidal cells (curved arrow) can be seen.

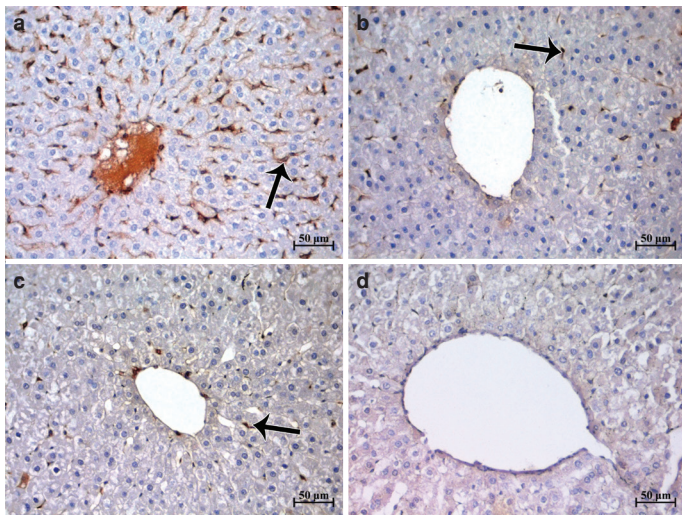


**Figure 4.** Representative micrographs of moesin in the (a) control, (b) diabetes, and (c) treatment groups, as well as (d) negative control. Moesin immunopositivity was observed predominantly in the hepatic sinusoidal cells (arrow). The immunopositivity ratio was significantly lower in the diabetes group and the treatment was ineffective.

ity decreased in the diabetes ( $6.01 \pm 2.64\%$ ) and treatment ( $6.40 \pm 2.10\%$ ) groups significantly ( $p < 0.01$ ), but the difference between these groups was not significant ( $p > 0.05$ ). A graphical demonstration of the radixin and moesin immunopositivity analyses is presented in Figure 5.

### Western Blotting Results

Immunoblotting intensity was measured by comparing the band intensity of a protein of interest using  $\beta$ -actin as a loading control. The results of the statistical analyses demonstrated that the radixin and moesin band intensity ratio of the control group was  $5.26 \pm 1.04$  and  $1.55 \pm 0.08$ , respectively. The ratios were  $4.64 \pm 1.25$  and  $0.64 \pm 0.24$ , respectively, in

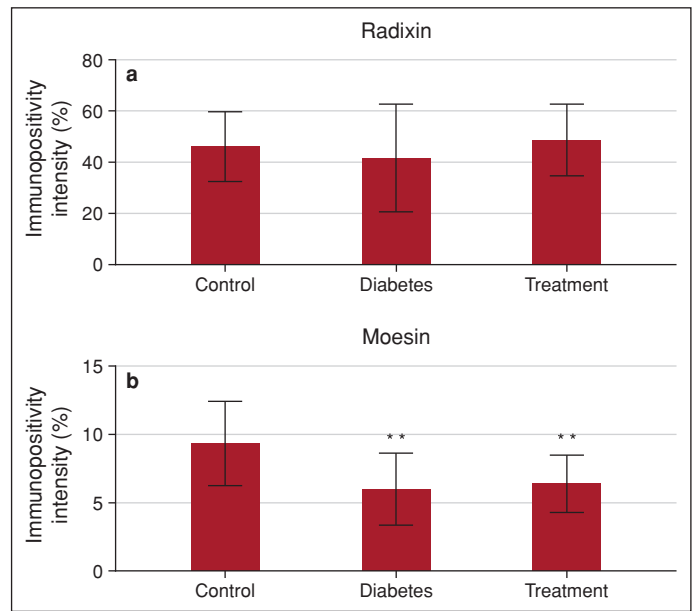


**Figure 5.** Graphical demonstration of (a) radixin and (b) moesin immunohistochemistry analyses.

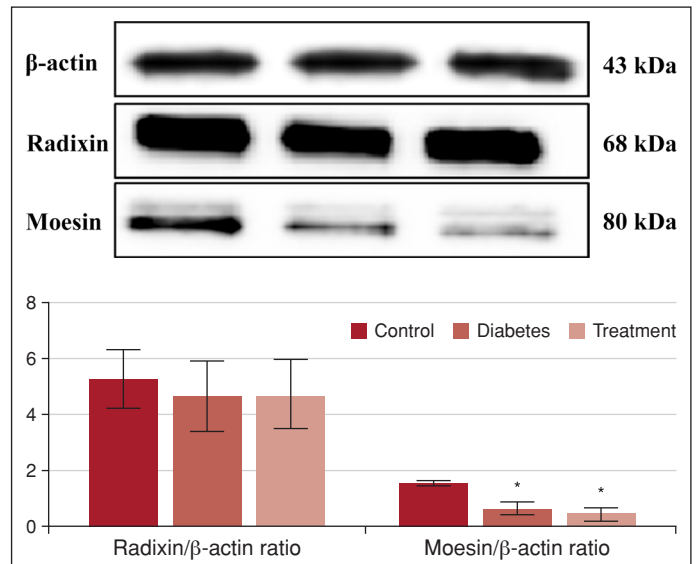


**Figure 6.** Demonstration of immunoblotting and statistical results of radixin and moesin expression in control, diabetes, and treatment groups. \*: Statistically significant difference between groups ( $p < 0.05$ ).

the diabetes group, and  $4.73 \pm 1.23$  and  $0.44 \pm 0.24$  in the group treated with black cummin oil. The intensity ratio of radixin between groups was similar ( $p > 0.05$ ), but the moesin ratio was significantly lower ( $p < 0.05$ ) in the diabetes and treatment groups (Fig. 6).

### Discussion

A minimum of 17% of diabetes patients are predicted to have liver disease.<sup>[20]</sup> Both clinical and experimental studies have demonstrated that oxidative stress plays a crucial role in diabetes-induced liver disease.<sup>[21]</sup> It has been reported that diabetes may be linked to upregulation of inflammatory cytokines and activation of adaptive and innate immune

cells linked to diabetic complications.<sup>[22]</sup> The primary cause of liver injury in diabetic patients is thought to be a result of hyperglycemia-induced oxidative stress and other complications of carbohydrate, lipid, and protein metabolism.<sup>[23]</sup> These complications boost the generation of excessive oxidative stress and the induction of inflammatory cascades. Widespread pathological changes, including structural degenerations, have been observed in cases of diabetes and increased oxidative stress.<sup>[8,24]</sup> It has also been reported that the oxidative stress may provoke cellular cytoskeleton actin depolymerization cross-linked to the cellular membrane by a group of proteins, ezrin-radixin-moesin (ERM).<sup>[25]</sup> In addition to the structural function, these proteins have been reported to contribute to cellular activities, such as cell migration, adhesion, cell polarization, motility, growth, fibrosis, and even membrane trafficking.<sup>[13,26]</sup> Although there are numerous previously published articles related to STZ-induced diabetic liver complications, the current literature regarding the potential influence of radixin and moesin in diabetes is very limited. It has been reported that increased hepatic DNA fragmentation was thought to be a result of oxidative and glycativ stress in STZ-induced diabetes.<sup>[27]</sup> Gosh et al.<sup>[28]</sup> found that STZ-induced diabetes provoked overexpression and activation of apoptotic proteins, such as p53, Bcl-2-associated X-protein, Bcl-XL/Bcl-2-associated death promoter, and cytochrome C. The authors concluded that the administration of the plant-derived antioxidant curcumin might be a successful strategy to protect the liver in STZ-induced experimental diabetes. Other studies have indicated that black cumin may function as an anti-hyperglycemic and antioxidant in STZ-induced diabetes.<sup>[29,30]</sup> The anti-fibrotic activity of this plant has also been noted in a carbon tetrachloride-induced experimental liver injury model.<sup>[31]</sup> Furthermore, Almatroodi et al.<sup>[32]</sup> investigated potential protective and anti-hyperglycemic effects of the most prominent constituent of black cumin, thymoquinone, against STZ-induced diabetes, and their results indicated that STZ increased the blood glucose level and upregulated the serum level of liver function enzymes and lipid peroxidation. The findings suggested that the administration of thymoquinone reduced diabetic complications in laboratory animals. Interestingly, intense collagen accumulation has been linked with greater fibrosis formation in insulin-independent diabetes compared with normal circumstances.<sup>[33]</sup>

It has been established that radixin is expressed in liver hepatocytes in healthy individuals, and is necessary to maintain hepatocyte apical canalicular membrane function and structure.<sup>[11,34]</sup> Kawase et al.<sup>[35]</sup> observed that radixin expression in the liver decreased in response to inflammation. Another recently published article also noted that moesin phosphorylation was upregulated during hepatic stellate cell activation and fibrogenesis in an experimental animal liver injury model.<sup>[13]</sup> Our immunostaining results regarding the cellular distribution of moesin in the liver were similar, however, our findings regarding the moesin expression level were somewhat different. The immunohistochemistry and immunoblotting results in our study indicated that moesin expression was significantly downregulated in an STZ-induced diabetic liver and upregulation was not observed in the rats treated with black cumin seed oil. The difference in the moesin level between the 2 studies might be a result of liver injury induction model. Karvar et al.<sup>[13]</sup> generated liver fibrosis model using administration of carbon tetrachloride and common bile duct ligation, while our study was designed with a STZ-induced diabetic liver model that rarely results in fibrosis.

There are some limitations to this study. First of all, we did not investigate the expression level of the third member of the ERM protein family, ezrin. Analysis of the expression level of all phosphorylated

proteins would provide more details. Previously published articles have also investigated just 1 or 2 members of the ERM protein family members while investigating the role of these proteins on various cellular mechanisms.<sup>[36,37]</sup> Nonetheless, our results provide some potentially valuable information about STZ-induced diabetic liver complications and potential contributions of these proteins to liver dysfunction as well as the effects of black cumin seed oil administration.

## Conclusion

To the best of our knowledge, this is the first study to investigate the expression of radixin and moesin in an STZ-induced diabetic rat liver and the effects of black cumin seed oil treatment. In brief, results of our study indicated that black cumin seed is a strong antioxidant. In addition, in tissue level the Radixin expression has not been changed, but Moesin expression reduced in STZ induced diabetic liver and black cumin seed oil treatment was failed. We believe the lack of significant response in moesin expression might be related to an inadequate dose or greater sensitivity of hepatic sinusoidal cells to diabetic complications.

**Ethics Committee Approval:** The Dicle University Local Experimental Animal Ethics Committee granted approval for this study (date: 28.03.2019, number: 2019/04).

**Author Contributions:** Concept – US, SK, YN; Design – US, SK; Supervision – SIK, DS, OUD, YN; Fundings – US, SK, YN; Materials – US, SK, SIK, DS, OUD; Data Collection and/or Processing – US, SIK, DS, OUD; Analysis and/or Interpretation – US, SIK; Literature Search – US, SK, SIK, DS, OUD, YN; Writing – US, SIK, DS; Critical Reviews – SIK, DS, OUD, YN.

**Conflict of Interest:** The authors have no conflict of interest to declare.

**Financial Disclosure:** This research was partially supported by Scientific Research Projects Coordinatorship of Dicle University (grant no: TIP.19.018).

## References

1. Cho N, Shaw J, Karuranga S, Huang Y, da Rocha Fernandes JD, Ohlrogge AW, et al. IDF Diabetes Atlas: Global estimates of diabetes prevalence for 2017 and projections for 2045. *Diabetes Res Clin Pract* 2018;138:271-281.
2. Amos AF, McCarty DJ, Zimmet P. The rising global burden of diabetes and its complications: estimates and projections to the year 2010. *Diabet Med* 1997;14(Suppl 5):S1-S85.
3. Harrison SA. Liver disease in patients with diabetes mellitus. *J Clin Gastroenterol* 2006;40(1):68-76.
4. Manna P, Das J, Ghosh J, Sil PC. Contribution of type 1 diabetes to rat liver dysfunction and cellular damage via activation of NOS, PARP, IkappaBalpha/NF-kappaB, MAPKs, and mitochondria-dependent pathways: Prophylactic role of arjunolic acid. *Free Radic Biol Med*. 2010 Jun 1;48(11):1465-1484.
5. Rodríguez V, Plavnik L, de Talamoni NT. Naringin attenuates liver damage in streptozotocin-induced diabetic rats. *Biomed Pharmacother* 2018;105:95-102.
6. Maksymchuk O, Shysh A, Rosohatska I, Chashchyn M. Quercetin prevents type 1 diabetic liver damage through inhibition of CYP2E1. *Pharmacol Rep* 2017;69(6):1386-1392.
7. Meral I, Yener Z, Kahraman T, Mert N. Effect of *Nigella sativa* on glucose concentration, lipid peroxidation, anti-oxidant defence system and liver damage in experimentally-induced diabetic rabbits. *J Vet Med A Physiol Pathol Clin Med* 2001;48(10):593-599.
8. Shimoni Y, Rattner JB. Type 1 diabetes leads to cytoskeleton changes that are reflected in insulin action on rat cardiac K(+) currents. *Am J Physiol Endocrinol Metab* 2001;281(3):E575-E585.

9. Neisch AL, Fehon RG. Ezrin, Radixin and Moesin: key regulators of membrane-cortex interactions and signaling. *Curr Opin Cell Biol* 2011;23(4):377-382.
10. Berryman M, Franck Z, Bretscher A. Ezrin is concentrated in the apical microvilli of a wide variety of epithelial cells whereas moesin is found primarily in endothelial cells. *J Cell Sci* 1993;105(Pt 4):1025-1043.
11. Ingraffea J, Reczek D, Bretscher A. Distinct cell type-specific expression of scaffolding proteins EBP50 and E3KARP: EBP50 is generally expressed with ezrin in specific epithelia, whereas E3KARP is not. *Eur J Cell Biol* 2002;81(2):61-68.
12. Kawaguchi K, Yoshida S, Hatano R, Asano S. Pathophysiological roles of ezrin/radixin/moesin proteins. *Biol Pharm Bull* 2017;40(4):381-390.
13. Karvar S, Ansa-Addo EA, Suda J, Singh S, Zhu L, Li Z, et al. Moesin, an ezrin/radixin/moesin family member, regulates hepatic fibrosis. *Hepatology* 2020;72(3):1073-1084.
14. Okayama T, Kikuchi S, Ochiai T, Ikoma H, Kubota T, Ichikawa D, et al. Attenuated response to liver injury in moesin-deficient mice: impaired stellate cell migration and decreased fibrosis. *Biochim Biophys Acta* 2008;1782(9):542-548.
15. Wasik AA, Koskelainen S, Hyvönen ME, Musante L, Lehtonen E, Koskeniemi K, et al. Ezrin is down-regulated in diabetic kidney glomeruli and regulates actin reorganization and glucose uptake via GLUT1 in cultured podocytes. *Am J Pathol* 2014;184(6):1727-1739.
16. Houcher Z, Boudiaf K, Benboubetra M, Houcher B. Effects of methanolic extract and commercial oil of *Nigella sativa* L. on blood glucose and antioxidant capacity in alloxan-induced diabetic rats. *Pteridines* 2007;18(1):8-18.
17. Mahmoud MR, El-Abhar HS, Saleh S. The effect of *Nigella sativa* oil against the liver damage induced by *Schistosoma mansoni* infection in mice. *J Ethnopharmacol* 2002;79(1):1-11.
18. Yagi K. Assay for blood plasma or serum. *Methods Enzymol* 1984;105:328-31.
19. Beutler E. Reduced glutathione (GSH). *Red Cell Metabolism* 1971:103-105.
20. Al-Hussaini AA, Sulaiman NM, Alzahrani MD, Alenizi AS, Khan M. Prevalence of hepatopathy in type 1 diabetic children. *BMC Pediatr* 2012;12:160.
21. Das J, Roy A, Sil PC. Mechanism of the protective action of taurine in toxin and drug induced organ pathophysiology and diabetic complications: a review. *Food Funct* 2012;3(12):1251-1264.
22. Devaraj S, Cheung AT, Jialal I, Griffen SC, Nguyen D, Glaser N, et al. Evidence of increased inflammation and microcirculatory abnormalities in patients with type 1 diabetes and their role in microvascular complications. *Diabetes* 2007;56(11):2790-2796.
23. Yazdi HB, Hojati V, Shiravi A, Hosseinian S, Vaezi G, Hadjzadeh MA. Liver dysfunction and oxidative stress in streptozotocin-induced diabetic rats: protective role of artemisia turanica. *J Pharmacopuncture* 2019;22(2):109-114.
24. Kohl T, Gehrke N, Schad A, Nagel M, Wörns MA, Sprinzl MF, et al. Diabetic liver injury from streptozotocin is regulated through the caspase-8 homolog cFLIP involving activation of JNK2 and intrahepatic immunocompetent cells. *Cell Death Dis* 2013;4(7):e712.
25. Allani PK, Sum T, Bhansali SG, Mukherjee SK, Sonnee M. A comparative study of the effect of oxidative stress on the cytoskeleton in human cortical neurons. *Toxicol Appl Pharmacol* 2004;196(1):29-36.
26. Louvet-Vallée S. ERM proteins: from cellular architecture to cell signaling. *Biology of the Cell* 2000;92(5):305-316.
27. Andican G, Burçak G. Oxidative damage to nuclear DNA in streptozotocin-diabetic rat liver. *Clin Exp Pharmacol Physiol* 2005;32(8):663-666.
28. Ghosh S, Bhattacharyya S, Rashid K, Sil PC. Curcumin protects rat liver from streptozotocin-induced diabetic pathophysiology by counteracting reactive oxygen species and inhibiting the activation of p53 and MAPKs mediated stress response pathways. *Toxicol Rep* 2015;2:365-376.
29. Fararh KM, Atoji Y, Shimizu Y, Shiina T, Nikami H, Takewaki T. Mechanisms of the hypoglycaemic and immunopotentiating effects of *Nigella sativa* L. oil in streptozotocin-induced diabetic hamsters. *Res Vet Sci* 2004;77(2):123-129.
30. Aisa H, Xin X, Tang D. *Nigella sativa*: A medicinal and edible plant that ameliorates diabetes. In: Watson R, Preedy V, editors. *Bioactive Food as Dietary Interventions for Diabetes*. Massachusetts: Academic Press; 2019:629-640.
31. Türkdoğan MK, Ağaoğlu Z, Yener Z, Sekeroğlu R, Akkan HA, Avcı ME. The role of antioxidant vitamins (C and E), selenium and *Nigella sativa* in the prevention of liver fibrosis and cirrhosis in rabbits: new hopes. *Dtsch Tierärztl Wochenschr* 2001;108(2):71-73.
32. Almatroodi SA, Alnuqaydan AM, Alsahli MA, Khan AA, Rahmani AH. Thymoquinone, the most prominent constituent of *nigella sativa*, attenuates liver damage in streptozotocin-induced diabetic rats via regulation of oxidative stress, inflammation and cyclooxygenase-2 protein expression. *Appl Sci* 2021;11(7):3223.
33. Lin CY, Adhikary P, Cheng K. Cellular protein markers, therapeutics, and drug delivery strategies in the treatment of diabetes-associated liver fibrosis. *Adv Drug Deliv Rev* 2021;174:127-139.
34. Wang W, Soroka CJ, Mennone A, Rahner C, Harry K, Pypaert M, Boyer JL. Radixin is required to maintain apical canalicular membrane structure and function in rat hepatocytes. *Gastroenterology* 2006;131(3):878-884.
35. Kawase A, Nakasaka M, Bando H, Yasuda S, Shimada H, Iwaki M. Changes in radixin expression and interaction with efflux transporters in the liver of adjuvant-induced Arthritic Rats. *Inflammation* 2020;43(1):85-94.
36. Clapéron A, Debray D, Redon MJ, Mergey M, Ho-Boulidoires TH, Housset C, Fabre M, Fouassier L. Immunohistochemical profile of ezrin and radixin in human liver epithelia during fetal development and pediatric cholestatic diseases. *Clin Res Hepatol Gastroenterol* 2013;37(2):142-151.
37. Okamura D, Ohtsuka M, Kimura F, Shimizu H, Yoshidome H, Kato A, et al. Ezrin expression is associated with hepatocellular carcinoma possibly derived from progenitor cells and early recurrence after surgical resection. *Modern Pathol* 2008;21(7):847-855.